# Supplemental Information

# The HAUS Complex Is a Key Regulator

# of Non-centrosomal Microtubule Organization

# during Neuronal Development

Inês Cunha-Ferreira, Anaël Chazeau, Robin R. Buijs, Riccardo Stucchi, Lena Will, Xingxiu Pan, Youri Adolfs, Christiaan van der Meer, Joanna C. Wolthuis, Olga I. Kahn, Philipp Schätzle, Maarten Altelaar, R. Jeroen Pasterkamp, Lukas C. Kapitein, and Casper C. Hoogenraad

**A**

Control

Pericentrin    α-Tubulin    DAPI

HAUS6 KD

Pericentrin  α-Tubulin  DAPI  HA-βGal

**B**

Mitotic index (%)

Control    HAUS6 KD

***

**C**

Abnormal spindles (%)

Control    HAUS6 KD

***

**D**

Control                                    Taxol 10 nM 48 hrs

Control    HAUS6 KD#1    HAUS6 KD#2          Control    HAUS6 KD#1    HAUS6 KD#2

GFP AnkG

AnkG

GFP Tau

Tau

**E**

DIV1

DIV5

DIV12

HAUS6 Centrin
MAP2

**F**

Normalized average intensity of HAUS6

ns

DIV0-1    DIV5    DIV12

**            *

DIV0-1    DIV5    DIV12

HAUS6

Centrin

**G**

Control          1    2

HAUS6 KD#1      1    2

HAUS6 KD#2      1    2

HAUS6 Centrin
HA-βGal

**H**

Normalized average intensity of HAUS6

Control    HAUS6 KD#1    HAUS6 KD#2

***          ***

**I**

Normalized average intensity of HAUS6

NT HAUS6 KD#1    HAUS6 KD#1    NT HAUS6 KD#2    HAUS6 KD#2
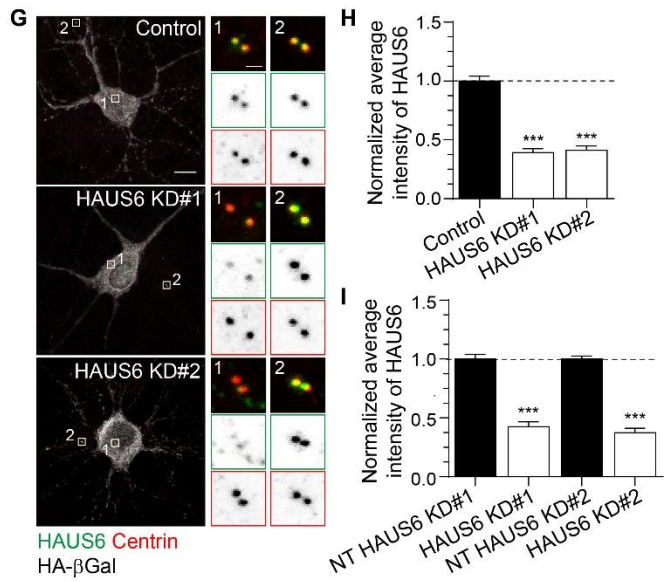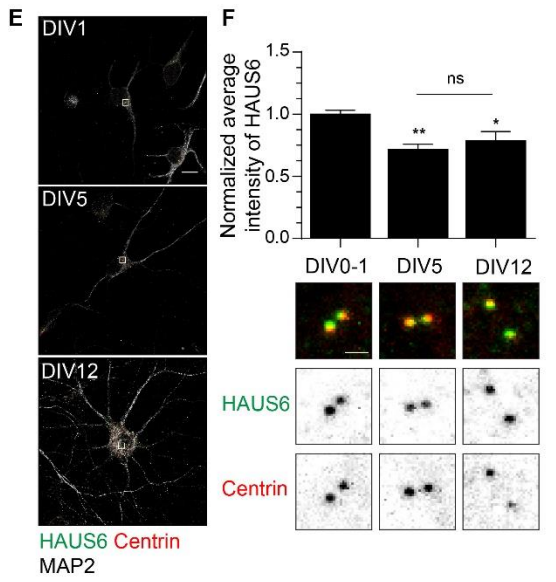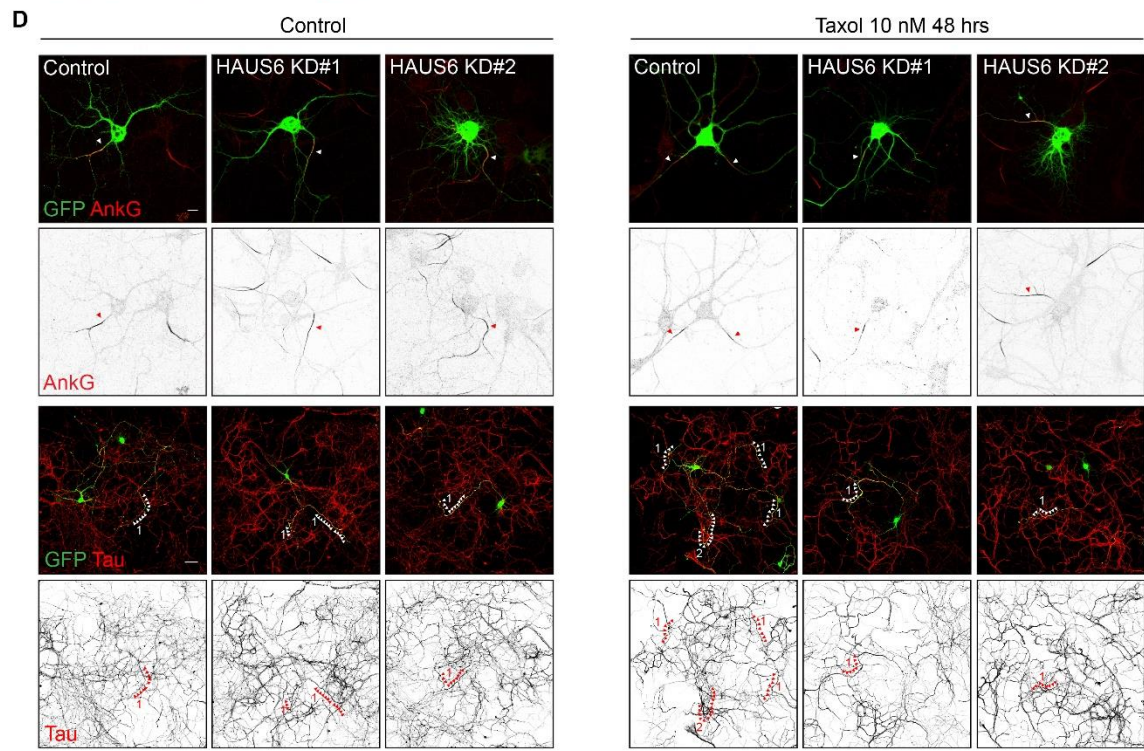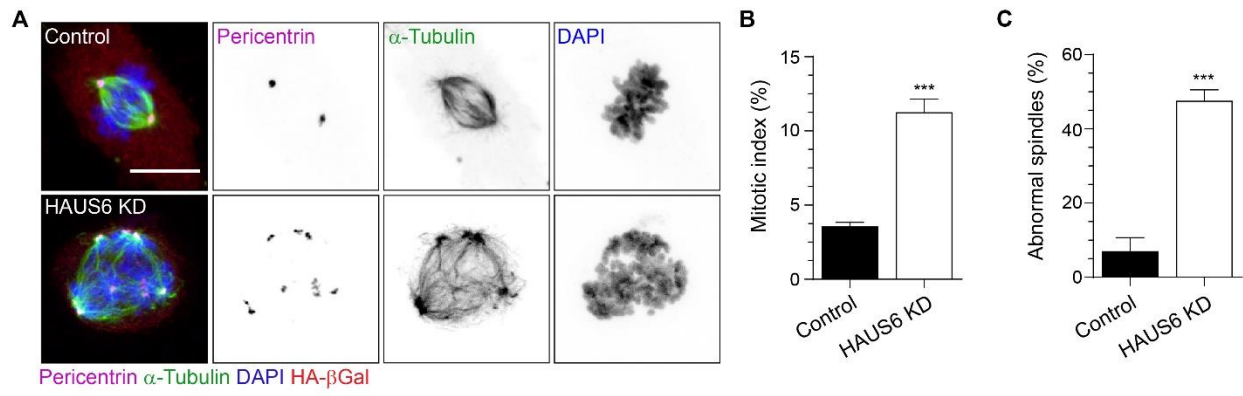
***                        ***

**Figure S1. The HAUS Complex is required for Neuronal Migration and Axon Specification, Related to Figure 1.**

**(A)** Maximum intensity projection of IMCD3 murine mitotic cells depleted of HAUS6 and pSuper control. Pericentrin (magenta), α-Tubulin (green), HA-β-galactosidase (red), DAPI (blue).

**(B, C)** Mitotic index (B) and percentage of abnormal mitotic spindles (C) after depletion of HAUS6 and pSuper control in IMCD3 cells (n=922-1206 in B, n=82-142 in C, N=3).

**(D)** DIV6 hippocampal neurons co-transfected with GFP and shRNAs for pSuper control, HAUS6 KD#1,2 at DIV2 and treated at DIV4 with control vehicle (DMSO) or Taxol. GFP (green) and AnkG or Tau (red). Processes positive for AnkG or Tau are indicated white arrowheads in merged images and red in gray-scale inverted images. Tau positive axons are numbered.

**(E)** Maximum intensity projections of DIV1, DIV5 and DIV12 hippocampal neurons labelled with HAUS6 (green), Centrin (red), MAP2 (gray).

**(F)** Normalized average intensity of HAUS6 at the centrosome in DIV0-1, DIV5 and DIV12 hippocampal neurons. Data normalized to DIV0-1 stage of development (n=23-24, N=2). Insets in F depict indicated areas in E.

**(G)** Maximum intensity projections of hippocampal neurons at DIV12 co-transfected with HA-β-galactosidase and shRNAs for HAUS6 KD#1, 2 or pSuper control. HAUS6 (green), Centrin (red), HA-β-galactosidase (gray). Inset #1 highlights the centrosome in a transfected cell and inset #2, the centrosome in a non-transfected cell.

**(H, I)** Normalized average intensity of HAUS6 related to G. Data was normalized to pSuper control in H (n=28-29, N=3) and to non-transfected cells (NT) within the same coverslip in I (n=28-30, N=3).

Graphs represent mean±SEM. $*p<0.05$, $**p<0.01$, $***p<0.001$. Scale bar 10 μm in A, E, G, 1 μm in F, G (centrosome panels), 10 μm in AnkG panels and 50 μm in Tau panels in D.
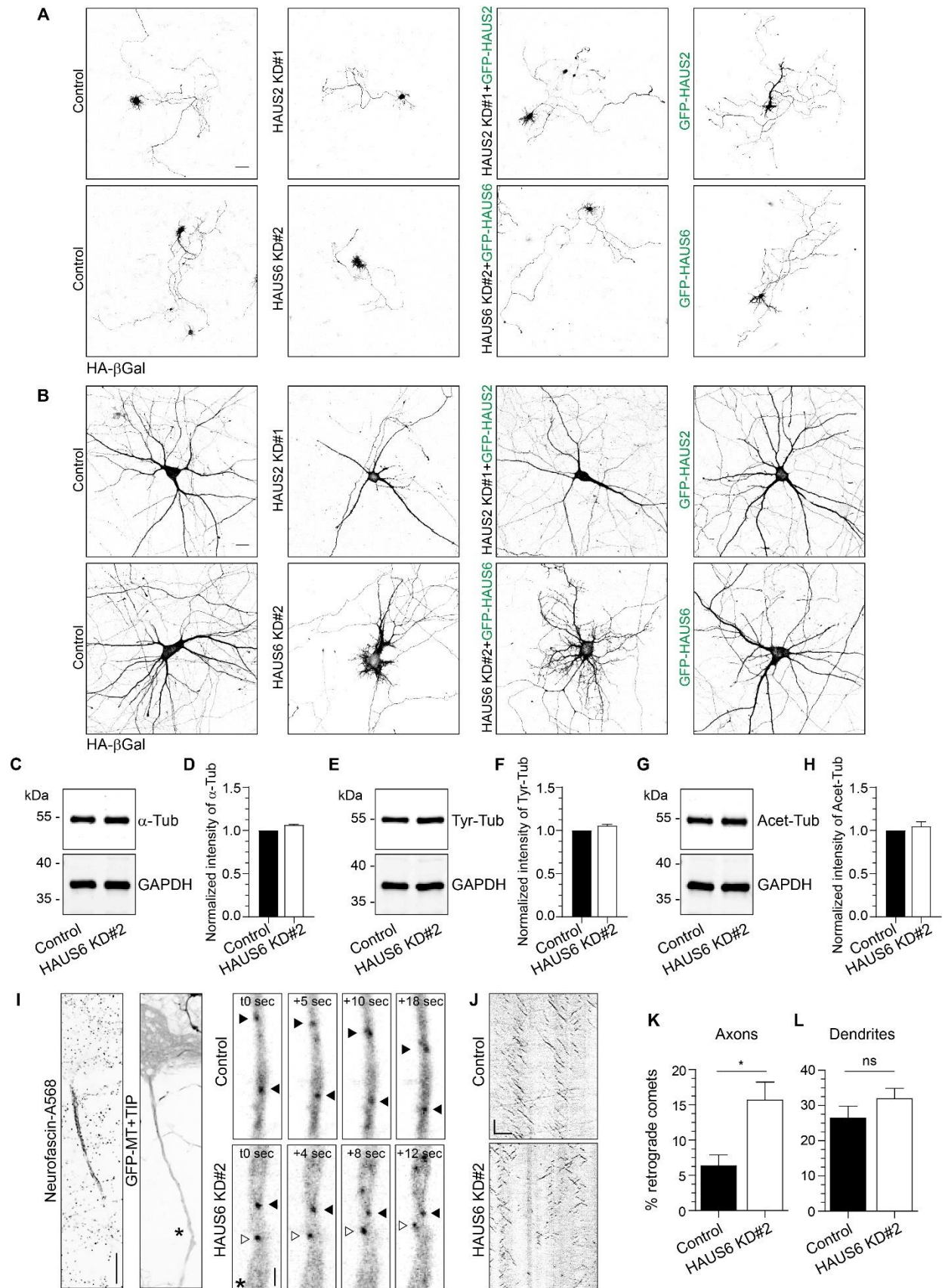
**A**

Control | HAUS2 KD#1 | HAUS2 KD#1+GFP-HAUS2 | GFP-HAUS2

Control | HAUS6 KD#2 | HAUS6 KD#2+GFP-HAUS6 | GFP-HAUS6

HA-βGal

**B**

Control | HAUS2 KD#1 | HAUS2 KD#1+GFP-HAUS2 | GFP-HAUS2

Control | HAUS6 KD#2 | HAUS6 KD#2+GFP-HAUS6 | GFP-HAUS6

HA-βGal

**C**

kDa
55 — α-Tub
40 —
35 — GAPDH

Control  HAUS6 KD#2

**D**

Normalized intensity of α-Tub

Control  HAUS6 KD#2

**E**

kDa
55 — Tyr-Tub
40 —
35 — GAPDH

Control  HAUS6 KD#2

**F**

Normalized intensity of Tyr-Tub

Control  HAUS6 KD#2

**G**

kDa
55 — Acet-Tub
40 —
35 — GAPDH

Control  HAUS6 KD#2

**H**

Normalized intensity of Acet-Tub

Control  HAUS6 KD#2

**I**

Neurofascin-A568 | GFP-MT+TIP | t0 sec | +5 sec | +10 sec | +18 sec

Control

t0 sec | +4 sec | +8 sec | +12 sec

HAUS6 KD#2

**J**

Control

HAUS6 KD#2

**K** Axons

% retrograde comets

*

Control  HAUS6 KD#2

**L** Dendrites

ns

Control  HAUS6 KD#2

**Figure S2. The HAUS Complex is Required for Neuronal Development and Microtubule Organization in Hippocampal Neurons, Related to Figure 2 and 3.**

**(A, B)** Images of DIV5 (A) and DIV12 (B) hippocampal neurons co-transfected with HA-β-galactosidase and pSuper control, HAUS2 KD#1 or HAUS6 KD#2 with GFP, GFP-HAUS2 or GFP HAUS6 (shRNA resistant).

**(C-H)** Cortical neurons electroporated with pSuper control and HAUS6 KD#2 shRNAs were analysed by western blot with α-Tubulin (C, D), tyrosinated tubulin (E, F), acetylated tubulin (G, H) and GAPDH antibodies (loading control). Quantification of normalized levels of α-Tubulin, tyrosinated tubulin and acetylated tubulin to the Control is shown in D, F and H respectively (N=2).

**(I, J)** Representative stills and kymographs of GFP-MT+TIP from 10 minute time lapse acquisitions of DIV11 neurons transfected with pSuper control and HAUS6 KD#2 shRNAs. Time is in seconds. Anterograde and retrograde growing MT+TIPs are indicated with black and white arrowheads, respectively. Extracellular labelling with Neurofascin-Alexa568 is used as an axon marker.

**(K, L)** Percentage of retrograde comets from data in I, J (n=16-30, N=4-5 in K and n=20-33, N=3 in L).

Graphs represent the mean±SEM. *$p<0.05$. Scale bar 50 μm in A, 20 μm in B, 10 μm in panels and 1 μm in stills in I, 5 μm and 1 minute in J.
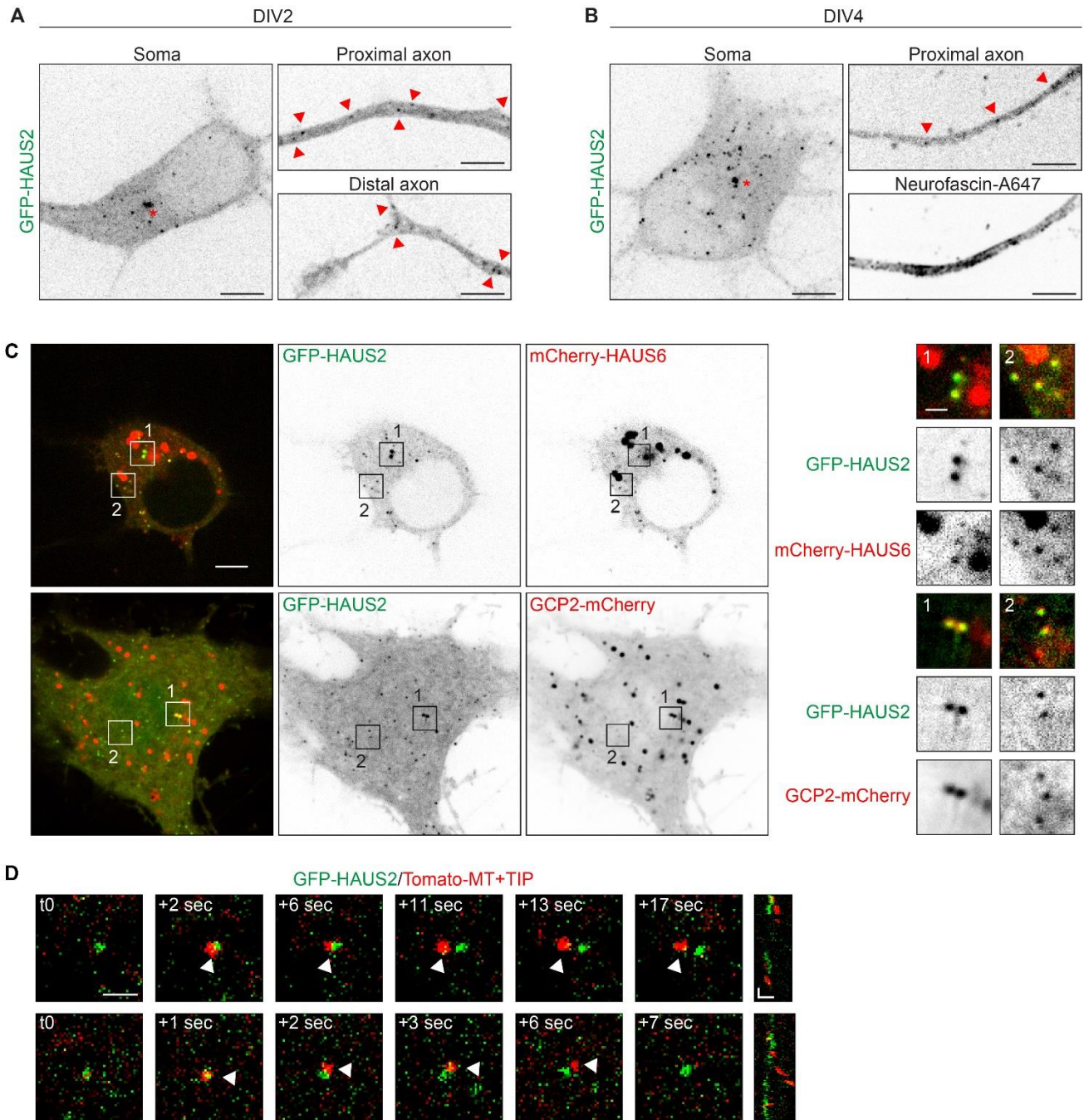
**Figure S3. Localization of GFP-HAUS2, HAUS6-mcherry and GCP2-mcherry in Hippocampal Neurons, Related to Figure 4.**

**(A)** Maximum intensity projection of a DIV2 neuron expressing GFP-HAUS2. The localization of GFP-HAUS2 clusters in proximal and distal axon is depicted in average projections of 10 frame acquisitions. GFP-HAUS2 localization at the centrosome is indicated with an asterisk and at non-centrosomal clusters along the axon with red arrowheads.

**(B)** Maximum intensity projection of a DIV4 neuron expressing GFP-HAUS2. The localization of GFP-HAUS2 clusters in proximal axon is depicted in average projections of 10 frame acquisitions. GFP-HAUS2 localization at the centrosome is depicted with an asterisk and non-centrosomal clusters along the axon with red arrowheads. Extracellular labelling with Neurofascin-Alexa647 was used as an axon marker.

**(C)** Average intensity projections of 10 frame stream acquisition of DIV10 hippocampal neurons co-transfected with GFP-HAUS2 (green) and mCherry-HAUS6 or GCP2-mCherry (red). Inset #1 indicates the centrosome and inset #2 the clusters outside the centrosome.

**(D)** Kymographs of 10 minute time lapse acquisitions of DIV17 neurons co-transfected with GFP-HAUS2 (green) and Tomato-MT+TIP (red).

Scale bar 5 μm in A, B, 5 μm in panels and 1 μm in insets in C, 1 μm in stills and 1 μm and 10 s in kymographs in D.

**A**

| Accession | Description | Bio-GFP #Peptides | Bio-GFP #PSM | Bio-GFP-HAUS2 #Peptides | Bio-GFP-HAUS2 #PSM | Bio-GFP-HAUS6 #Peptides | Bio-GFP-HAUS6 #PSM |
|---|---|---|---|---|---|---|---|
| Q96CS2 | HAUS1 | | | 6 | 7 | 6 | 7 |
| Q9NVX0 | HAUS2 | | | 21 | 235 | 5 | 7 |
| Q68CZ6 | HAUS3 | | | 14 | 19 | 10 | 17 |
| Q9H6D7 | HAUS4 | | | 15 | 24 | 6 | 9 |
| O94927 | HAUS5 | | | 22 | 36 | 20 | 28 |
| Q7Z4H7 | HAUS6 | | | 14 | 22 | 54 | 306 |
| Q99871 | HAUS7 | | | 7 | 14 | 6 | 13 |
| Q9BT25 | HAUS8 | | | 4 | 4 | 5 | 6 |

**B**

HEK293
HEK293 + Brain
Brain

HEK293
HEK293 + Brain
Brain

**C**

Actin cytoskeleton
Microtubule cytoskeleton
Cytoskeleton

Bio-GFP-HAUS2
Bio-GFP-HAUS6

Group occurence within significant interactors (%)

**D**

Brain

Microtubule-binding — Actin-binding

gene name

# peptides
0 20 40 60 80 100

log2 PSMs bait/GFP

log2 PSMs bait/GFP

**E**

HEK293

Microtubule-binding — Actin-binding

# peptides
0 10 20 30 40 50

log2 PSMs bait/GFP

log2 PSMs bait/GFP

**F**

GFP-HAUS2 LifeAct-GFP αTub-A647

**G**

% of GFP-HAUS2 clusters

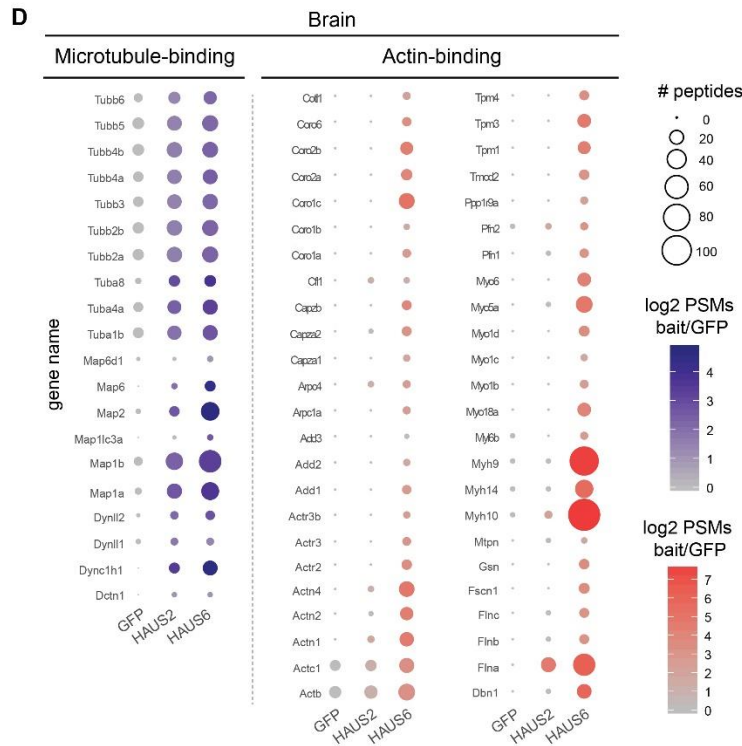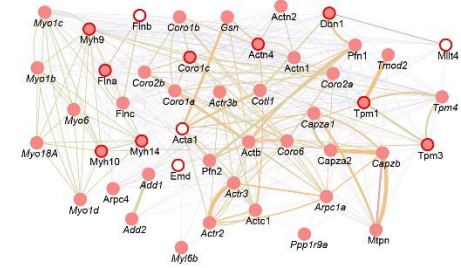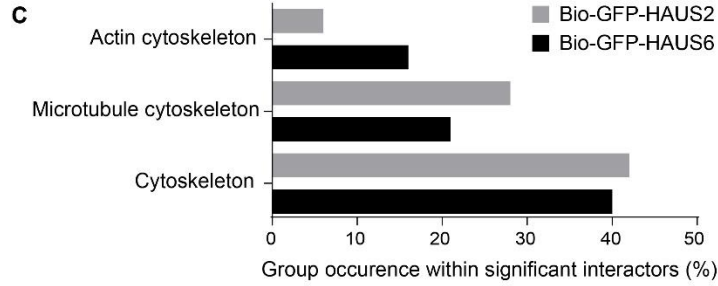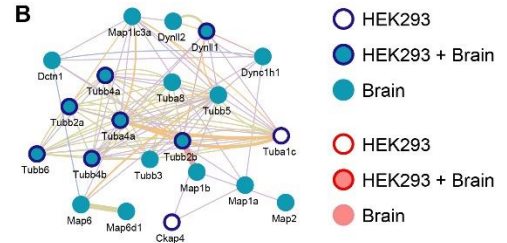| Microtubules | - | + | - | + |
| F-actin | - | - | + | + |
| | 1 | 2 | 3 | 4 |

**Figure S4. HAUS2 and HAUS6 Interact with Microtubule and Actin Binding Proteins in Brain, Related to Figure 4.**
**(A)** HAUS binding partners of Bio-GFP-HAUS2 and HAUS6 in HEK293 cells identified by AP-MS.
**(B)** Network analysis on HAUS2 and 6 putative binding partners associated with the microtubule (blue) and actin cytoskeleton (red). Edge color coding: blue, colocalization; orange, predicted interaction; green, shared protein domain; purple, co-expression.
**(C)** Subset of Gene Ontology classifiers (actin cytoskeleton, microtubule cytoskeleton and cytoskeleton) overrepresented in HAUS2 (grey) or HAUS6 (black) significant interactors in adult rat bains.
**(D, E)** Selected putative binding partners of Bio-GFP-HAUS2 and HAUS6 identified in adult rat brains (D) and HEK293 (E) by AP-MS. The peptide count is graphically represented by spheres, the ratio of the spectral counts of the bait over the control is represented in blue for microtubule binding proteins and red for actin binding proteins.
**(F)** Single molecule super-resolution reconstruction of a DIV4 hippocampal neuron transfected with GFP-HAUS2 (red), extracted and fixed with GA and PFA, and post-labelled with LifeAct-GFP (cyan) and DNA-PAINT (yellow) to visualize actin and α-Tubulin, respectively. Insets depict indicated areas.
**(G)** Percentage of GFP-HAUS2 clusters across 4 different categories: 1 – No colocalization, 2 – colocalization with microtubules, 3 – colocalization with actin and 4 – colocalization with microtubules and actin. (n=3, N=1).
Data is presented as mean±SD. Scale bar 2 μm in panel and 500 nm in insets in F.


**Supplemental Tables**


**Table S1. Overview of the Data and Statistical Analysis in this Study, Related to Figure 1-4 and Figure S1, S2 and S4.**

| Figure | Sample size (n) | N | Statistical test | Values |
|---|---|---|---|---|
| 1B | Control = 15 slices<br>HAUS6 KD = 16 slices | 6 ($\geq$ 3litters)<br>6 ($\geq$ 3litters) | Mann Whitney U test | Control x HAUS6 KD bin 20: U = 11, p = 0.3095<br>Control x HAUS6 KD bin 40: U = 5, p = 0.0411<br>Control x HAUS6 KD bin 60: U = 13, p = 0.4848<br>Control x HAUS6 KD bin 80: U = 8, p = 0.1320<br>Control x HAUS6 KD bin 100: U = 4, p = 0.0260 |
| 1D | Control = 5 slices (51 neurons)<br>HAUS6 KD = 6 slices (92 neurons) | 3 (2 litters)<br>3 (2 litters) | Mann Whitney U test | U = 0, p = 0.0043 |
| 1E | Control = 5 slices (51 neurons)<br>HAUS6 KD = 6 slices (92 neurons) | 3 (2 litters)<br>3 (2 litters) | Mann Whitney U test | U = 0, p = 0.0043 |
| 1F | Control = 5 slices (51 neurons)<br>HAUS6 KD = 6 slices (92 neurons) | 3 (2 litters)<br>3 (2 litters) | Mann Whitney U test | Type 1: U = 0, p = 0.0043<br>Type 2: U = 0, p = 0.0043<br>Type 3: U = 1.500, p = 0.0108<br>Type 4: U = 4, p = 0.0498 |
| 1H | Control TRIM46 = 32<br>Control AnkG = 34<br>Control Tau = 19<br>HAUS6 KD#1TRIM46 = 32<br>HAUS6 KD#1 AnkG = 34<br>HAUS6 KD#1 Tau = 21<br>HAUS6 KD#2 TRIM46 = 32<br>HAUS6 KD#2 AnkG = 34<br>HAUS6 KD#2 Tau = 22 | 3<br>3<br>2<br>3<br>3<br>2<br>3<br>3<br>2 | Kruskal-Wallis test Dunn's multiple comparisons test | Kruskal-Wallis test<br>H ($\chi^2$) = 8.993; p = 0.3429<br>Dunn's multiple comparisons test<br>TRIM46 - Control x HAUS6 KD#1: p > 0.9999<br>TRIM46 - Control x HAUS6 KD#2: p > 0.9999<br>AnkG - Control x HAUS6 KD#1: p > 0.9999<br>AnkG - Control x HAUS6 KD#2: p > 0.9999<br>Tau - Control x HAUS6 KD#1: p > 0.9999<br>Tau - Control x HAUS6 KD#2: p > 0.9999 |
| 1I | Control TRIM46 = 31<br>Control AnkG = 34<br>Control Tau = 18<br>HAUS6 KD#1 TRIM46 = 30<br>HAUS6 KD#1 AnkG = 33<br>HAUS6 KD#1 Tau = 20<br>HAUS6 KD#2 TRIM46 = 31<br>HAUS6 KD#2 AnkG = 32<br>HAUS6 KD#2 Tau = 22 | 3<br>3<br>2<br>3<br>3<br>2<br>3<br>3<br>2 | Kruskal-Wallis test Dunn's multiple comparisons test | Kruskal-Wallis test<br>H ($\chi^2$) = 84.88; p < 0.0001<br>Dunn's multiple comparisons test<br>TRIM46 - Control x HAUS6 KD#1: p = 0.0029<br>TRIM46 - Control x HAUS6 KD#2: p < 0.0001<br>AnkG - Control x HAUS6 KD#1: p = 0.0003<br>AnkG - Control x HAUS6 KD#2: p < 0.0001<br>Tau - Control x HAUS6 KD#1: p = 0.0021<br>Tau - Control x HAUS6 KD#2: p < 0.0001 |
| 2B | Control = 19<br>γ-Tub KD = 20<br>HAUS2 KD#1 = 18<br>HAUS2 KD#2 = 20<br>HAUS6 KD#1 = 20<br>HAUS6 KD#2 = 20 | 2<br>2<br>2<br>2<br>2<br>2 | One Way ANOVA Holm-Sidak's multiple comparisons test | One Way ANOVA<br>F (DFn, DFd) = F (5, 111) = 17.59, p < 0.0001<br>Holm-Sidak's multiple comparisons test<br>Control x γ-Tub KD: p < 0.0001<br>Control x HAUS2 KD#1: p < 0.0001<br>Control x HAUS2 KD#2: p < 0.0001<br>Control x HAUS6 KD#1: p < 0.0001 |

| | | | | |
|---|---|---|---|---|
| | | | | Control x. HAUS6 KD#2: p < 0.0001 |
| **2C** | Control = 24<br>GFP-HAUS2 = 20<br>HAUS2 KD#1 = 21<br>HAUS2 KD#1 + GFP-HAUS2 = 18 | 2<br>2<br>2<br>2 | One Way ANOVA Holm-Sidak's multiple comparisons test | <u>One Way ANOVA</u><br>F (DFn, DFd) = F (3, 79) = 15.36, p < 0.0001<br><u>Holm-Sidak's multiple comparisons test</u><br>Control x GFP-HAUS2: p = 0.2334<br>Control x HAUS2 KD#1: p < 0.0001<br>Control x HAUS2 KD#1 + GFP-HAUS2: p = 0.1556<br>GFP-HAUS2 x HAUS2 KD#1: p < 0.0001<br>GFP-HAUS2 x HAUS2 KD#1 + GFP-HAUS2: p = 0.0184<br>HAUS2 KD#1 x HAUS2 KD#1 + GFP-HAUS2: p = 0.0064 |
| **2D** | Control = 21<br>GFP-HAUS6 = 19<br>HAUS6 KD#2 = 20<br>HAUS6 KD#2 + GFP-HAUS6 = 22 | 2<br>2<br>2<br>2 | One Way ANOVA Holm-Sidak's multiple comparisons test | <u>One Way ANOVA</u><br>F (DFn, DFd) = F (3, 78) = 18.68, p < 0.0001<br><u>Holm-Sidak's multiple comparisons test</u><br>Control x GFP-HAUS6: p = 0.4121<br>Control x HAUS6 KD#2: p < 0.0001<br>Control x HAUS6 KD#2 + GFP-HAUS6: p = 0.1387<br>GFP-HAUS6 x HAUS6 KD#2: p < 0.0001<br>GFP-HAUS6 x HAUS6 KD#2 + GFP-HAUS6: p = 0.0321<br>HAUS6 KD#2 x HAUS6 KD#2 + GFP-HAUS6: p = 0.0001 |
| **2F,G** | Control = 46<br>γ-Tubulin = 46<br>HAUS2 KD#1 = 20<br>HAUS2 KD#2 = 23<br>HAUS6 KD#1 = 20<br>HAUS6 KD#2 = 22 | 2<br>2<br>2<br>2<br>2<br>2 | | |
| **2H** | Control = 20<br>GFP-HAUS2 = 20<br>HAUS2 KD#1 = 20<br>HAUS2 KD#1 + GFP-HAUS2 = 20 | 2<br>2<br>2<br>2 | | |
| **2I** | Control = 30<br>GFP-HAUS6 = 30<br>HAUS6 KD#2 = 30<br>HAUS6 KD#2 + GFP-HAUS6 = 30 | 3<br>3<br>3<br>3 | | |
| **2J** | Control = 46<br>γ-Tubulin = 46<br>HAUS2 KD#1 = 20<br>HAUS2 KD#2 = 23<br>HAUS6 KD#1 = 20<br>HAUS6 KD#2 = 22 | 2<br>2<br>2<br>2<br>2<br>2 | Two Way ANOVA Dunnett's multiple comparisons test | <u>Two Way ANOVA</u><br>Interaction: F (DFn, DFd) = F (50, 1881) = 2.991, p < 0.0001<br>Distance: F (DFn, DFd) = F (10, 1881) = 55.47, p < 0.0001<br>Sample: F (DFn, DFd) = F (5, 1881) = 38.05, p < 0.0001<br><u>Dunnett's multiple comparisons test</u><br>Control x γ-Tubulin: p < 0.0001<br>Control x HAUS2_KD#1: p < 0.0001<br>Control x HAUS2_KD#2: p < 0.0001<br>Control x HAUS6_KD#1: p = 0.0368<br>Control x HAUS6_KD#2: p < 0.0001 |
| **2K** | Control = 20<br>HAUS2 KD#1 = 20<br>GFP-HAUS2 = 20<br>HAUS2 KD#1 + GFP-HAUS2 = 20 | 2<br>2<br>2<br>2 | Two Way ANOVA Tukey's multiple comparisons test | <u>Two Way ANOVA</u><br>Interaction: F (DFn, DFd) = F (30, 836) = 1.751, p = 0.0080<br>Distance: F (DFn, DFd) = F (10, 836) = 20.06, p < 0.0001<br>Sample: F (DFn, DFd) = F (3, 836) = 104.1, p < 0.0001<br><u>Tukey's multiple comparisons test</u><br>Control x HAUS2 KD#1: p < 0.0001<br>Control x GFP-HAUS2: p = 0.9912<br>Control x HAUS2 KD#1 + GFP-HAUS2: p = 0.0281<br>HAUS2 KD#1 x GFP-HAUS2: p < 0.0001<br>HAUS2 KD#1 x HAUS2 KD#1 + GFP-HAUS2: p = 0.0026<br>GFP-HAUS2 x HAUS2 KD#1 + GFP-HAUS2: p = 0.0620 |
| **2L** | Control = 30<br>HAUS6 KD#2 = 30<br>GFP-HAUS6 = 30<br>HAUS6 KD#2 + GFP-HAUS6 = 30 | 3<br>3<br>3<br>3 | Two Way ANOVA Tukey's multiple comparisons test | <u>Two Way ANOVA</u><br>Interaction: F (DFn, DFd) = F (30, 1276) = 15.97, p < 0.0001<br>Distance: F (DFn, DFd) = F (10, 1276) = 38.29, p < 0.0001<br>Sample: F (DFn, DFd) = F (3, 1276) = 35.20, p < 0.0001<br><u>Tukey's multiple comparisons test</u><br>Control x HAUS6 KD#2: p = 0.0009<br>Control x GFP-HAUS6: p = 0.3251<br>Control x HAUS6 KD#2 + GFP-HAUS6: p = 0.9813<br>HAUS6 KD#2 x GFP-HAUS6: p = 0.1562<br>HAUS6 KD#2 x HAUS6 KD#2 + GFP-HAUS6: p = 0.0002<br>GFP-HAUS6 x HAUS6 KD#2 + GFP-HAUS6: p = 0.1608 |
| **3B** | Control = 20<br>HAUS6 KD#2 = 20 | 2<br>2 | Two tailed unpaired t-test | t = 5.808, df = 38, p < 0.0001 |

| | | | | |
|---|---|---|---|---|
| **3C** | Control = 20<br>HAUS6 KD#2 = 20 | 2<br>2 | Mann Whitney U test | U = 78, p = 0.0007 |
| **3E** | Control = 17<br>HAUS6 KD#2 = 17 | 2<br>2 | Two tailed unpaired t-test | t = 3.209, df = 32, p = 0.0030 |
| **3G** | Control = 19<br>HAUS6 KD#2 = 17 | 2<br>2 | Mann Whitney U test | U = 92.50, p = 0.0281 |
| **3H** | Control = 19<br>HAUS6 KD#2 = 17 | 2<br>2 | Two tailed unpaired t-test | t = 3.619, df = 34, p = 0.0010 |
| **4B** | GFP-HAUS2/mCherry-HAUS6 = 28<br>GFP-HAUS2/GCP2-mCherry = 51 | 4<br>4 | | |
| **4D** | Control = 43<br>HAUS6 KD#2 = 43 | 2<br>2 | Mann Whitney U test | U = 488, p = 0.0001 |
| **4G** | GFP-HAUS2 = 23 neurons, 24 dendrites (485 events) | 3 | Two tailed unpaired t-test | t = 12.95, df = 46, p < 0.0001 |
| **4H** | GFP-HAUS2 = 21 neurons, 22 dendrites (129 events) | 3 | Two tailed unpaired t-test | t = 0.1418, df = 42, p = 0.8879 |
| **4I** | GFP-HAUS2 = 21 neurons, 22 dendrites (129 events) | 3 | | |
| **4J** | GFP-HAUS2 = 21 neurons, 22 dendrites (129 events) | 3 | | |
| **S1B** | Control = 1206<br>HAUS6 KD = 922 | 3<br>3 | Two-tailed Chi-square with Yates' correction | $\chi^2$, df (46.40, 1), p < 0.0001 |
| **S1C** | Control = 82<br>HAUS6 KD = 142 | 3<br>3 | Two-tailed Fisher's exact test | p < 0.0001 |
| **S1F** | DIV0-1 = 23<br>DIV5 = 24<br>DIV12 = 24 | 2<br>2<br>2 | One Way ANOVA Tukey's multiple comparisons test | One Way ANOVA<br>F (DFn, DFd) = F (2, 68) = 7.664, p = 0.0010<br>Tukey's multiple comparisons test<br>DIV0-1 x DIV5: p = 0.0010<br>DIV0-1 x DIV12: p = 0.0158<br>DIV5 x DIV12: p = 0.6264 |
| **S1H** | Control = 29<br>HAUS6 KD#1 = 28<br>HAUS6 KD#2 = 29 | 3<br>3<br>3 | One-way ANOVA Dunnett's multiple comparisons test | One Way ANOVA<br>F (DFn, DFd) = F (2, 83) = 79.86, p < 0.0001<br>Dunnett's multiple comparisons test<br>Control x HAUS6 KD#1: p < 0.0001<br>Control x HAUS6 KD#2: p < 0.0001 |
| **S1I** | NT HAUS6 KD#1 = 30<br>HAUS6 KD#1 = 28<br>NT HAUS6 KD#2 = 30<br>HAUS6 KD#2 = 29 | 3<br>3<br>3<br>3 | One-way ANOVA Sidak's multiple comparisons test | One-way ANOVA<br>F (DFn, DFd) = F (3, 113) = 89.42, p < 0.0001<br>Sidak's multiple comparisons test<br>NT HAUS6 KD#1 x HAUS6 KD#1: p < 0.0001<br>NT HAUS6 KD#2 x HAUS6 KD#2: p < 0.0001 |
| **S2D,F,H** | | 2 | | |
| **S2K** | Control = 16<br>HAUS6 KD#2 = 30 | 4<br>5 | Mann Whitney U test | U = 138, p = 0.0175 |
| **S2L** | Control = 20<br>HAUS6 KD#2 = 33 | 3<br>3 | Two tailed unpaired t-test | t = 1.200, df=51, p = 0.2357 |
| **S4G** | 3 | 1 | | |

## Supplemental Experimental Procedures

Further information and requests for resources and reagents should be directed to and will be fulfilled by the Lead Contact Casper Hoogenraad (c.hoogenraad@uu.nl).

## Animals

All experiments were approved by the Dutch Animal Experiments Committee (Dier Experimenten Commissie [DEC]), performed in line with institutional guidelines of University Utrecht and UMC (University Medical Center) Utrecht and conducted in agreement with Dutch law (*Wet op de Dierproeven*, 1996) and European regulations (Directive 2010/63/EU). Female pregnant C57BL/6J mice were obtained from The Jackson Laboratory and female pregnant Wistar rats from Janvier. Both species were aged at least 10 weeks at the time of delivery. Upon delivery, mice and rats were kept in a controlled 12 hrs light-dark cycle with a temperature of $22 \pm 1°C$ and were given unrestricted access to food and water. The animals were housed with companions in transparent plexiglas cages with wood-chip bedding and paper tissue for nest building and cage enrichment. For *in utero* electroporation experiments, embryos of both genders were used at E14.5 stage of development. For hippocampal and cortical neuron culture experiments obtained from rat embryos, embryos of both genders at E18 stage of development were used. None of the parameters analysed in this study are reported to be affected by embryo gender. The animals, pregnant females and embryos have not been involved in previous procedures.

## Cell lines

HEK293 female cells (CRL1573) and mouse inner medullary collecting duct 3 (IMCD3) cells (CRL2123) were purchased from American Type Culture Collection (ATCC). The sex is undetermined for the IMCD3 cell line. Cell lines were not authenticated by authors after purchase. Both cell lines were cultured in DMEM/Ham's F10 (45%/45%) supplemented with 10% FCS and 1% penicillin/streptomycin at 37°C and 5% $CO_2$ and seeded on 18 mm glass coverslips prior to transfection, or in 10 cm dishes for biochemistry experiments.

## Primary neuronal cultures, transfection and electroporation

Primary hippocampal and cortical cultures were prepared from E18 rat brains (both genders) by mechanical and enzymatic dissociation (Goslin and Banker, 1989; Kapitein et al., 2010b). Hippocampal neurons were plated on coverslips coated with poly-L-lysine (37.5 μg/mL, Sigma) and laminin (1.25 μg/mL, Roche Diagnostics) at a density of 100,000 cells/well. Hippocampal neurons were transfected using Lipofectamine 2000 (Invitrogen). Briefly, DNA (1.8 μg/well in a 12 well plate) was mixed with 3.3 μL of Lipofectamine 2000 in 200 μL NB, incubated for 30 minutes, and then added to the neurons in NB with 0.5 mM glutamine at 37°C in 5% $CO_2$ for 45 minutes to 1 hr. Next, neurons were washed with NB and transferred in the original medium at 37°C in 5% $CO_2$ for 24-48 hrs (for overexpression) or 96 hrs (for shRNA expression). Primary cortical neurons were electroporated ($1,2x10^6$ cells per sample) using the Amaxa Rat Neuron Nucleofector kit (Lonza) with 3μg of DNA and plated in 6-well plates. Cells were grown at 37°C in 5% CO2 for 96 hrs prior to western blot analysis. Hippocampal and cortical neurons were cultured in Neurobasal medium (NB, GIBCO) supplemented with 2% B27 (GIBCO), 0.5 mM glutamine (GIBCO), 15.6 μM glutamate (Sigma-Aldrich) and 1% penicillin–streptomycin (GIBCO).

## *In utero* electroporation

*In utero* electroporation was performed as described previously (van Beuningen et al., 2015). Briefly, pregnant C57BL/6J mice were anaesthetized with Isoflurane (induction: 3-4%, surgery: 1.5-2%) at E14.5 and injected with 0.05 mg/kg buprenorfinhydrochloride in saline. The abdominal cavity was opened under sterile surgical conditions and uterine horns were exposed. 1.7 μL DNA mixture containing 0.6 μg/μL pSuper vector as control or a mix of two mouse HAUS6 shRNAs and 0.4 μg/μL GFP vector dissolved in MilliQ water with 0.05% Fast Green (Sigma) was injected in the lateral ventricles of the embryo using glass micro-pipettes (Harvard Apparatus) and a PLI-100 Picoinjector (Harvard Apparatus). Brains (motor cortex) were electroporated with gold plated tweezer-electrodes (Fisher Scientific) using an ECM 830 Electro-Square-Porator (Harvard Apparatus) set to 5 unipolar pulses at 30V (95 ms interval and 50 ms pulse length). Embryos were placed back into the abdomen, and abdominal muscles and skin were sutured separately. Mother mice were awakened by releasing them from Isoflurane. The welfare of the mother mice was controlled daily. Embryonic brains were collected at E17.5 and processed for immunohistochemistry.

## Heterologous cell culture and transfection

HEK293 cells were transfected with polyethylenimine (1 μg/μL) (PEI, Polysciences) and IMCD3 with Lipofectamine 2000 (Invitrogen) according to manufacturer's protocol. Coverslips with transfected IMCD3 cells were fixed and used for immunocytochemistry and HEK293 were processed for biochemistry experiments.

## DNA and shRNA constructs

The following mammalian expression vectors have been described: pGW1 (Hoogenraad et al., 2005), pGW2 and pβactin (Kapitein et al., 2010a), pGW2-BFP (Tortosa et al., 2017), pβactin-HA-β-galactosidase (Hoogenraad et al., 2005), pSuper vector (Brummelkamp et al., 2002), Bio-GFP vector (Jaworski et al., 2009), BirA vector was a kind gift from Dr. D. Meijer

(Erasmus MC, Rotterdam, The Netherlands). p-Syn-TdTomato-MACF18 which we named Tomato-MT+TIP was used as a general marker of microtubule growing plus ends. Briefly, the vector was generated by replacing the CMV promoter and intron sequence of GW2 (MluI/HindIII) with the 0.5 kb rat Synapsin promoter (Dittgen et al., 2004). Tomato-MACF18 is identical to GFP-MACF18 (Schatzle et al., 2016) except for the exchange of GFP to tandem dimer Tomato. The GFP-MT+TIP construct used in live-imaging experiments to track polymerizing ends of microtubules was p-Syn-GFP-MACF18 (with Synapsin promoter) generated using published strategy to reduce expression levels, since we used it in conjunction with shRNA expressed for 96 hrs (Ferreira et al., 2013). Upstream open reading frame containing a Kozak sequence was introduced before the start codon of GFP in the synGFP-MACF18 construct. Depending on Kozak sequence strength, a certain percent of the ribosomes are expected to initiate translation here and disassemble once they reach the stop codon, therefore the number of ribosomes that can translate the gene of interest is lowered and expression becomes significantly reduced. The Kozak sequence used was gggATGGGTTAAGGCCTaccATG. pGW2-GFP, pGW2-mRFP and pGW2-mCherry were created by inserting each tag in HindIII/AscI sites of a pGW2 vector. Full length human HAUS2 RefSeq 235 aa isoform (NCBI:NM_018097.2, UniProt:Q9NVX0) was amplified by PCR from pEGFP-C1-HAUS2 (a kind gift from Dr. Laurence Pelletier, Lunenfeld-Tanenbaum Research Institute, Mount Sinai Hospital, Toronto, Canada) and inserted in AscI/SalI sites of pGW2-GFP expression vector. To generate pGW2-GFP-HAUS6 the full length RefSeq 955 aa isoform (NCBI:NM_017645, UniProt:Q7Z4H7) was amplified by PCR from pEGFP-C1-HAUS6 (a kind gift from Dr. Laurence Pelletier, Lunenfeld-Tanenbaum Research Institute, Mount Sinai Hospital, Toronto, Canada) and inserted in AscI/SalI restriction sites of pGW2-GFP vector. pGW2-mCherry-HAUS6 was generated by recloning HAUS6 from pGW2-GFP-HAUS6 with AscI/SalI restriction sites and ligation with pGW2-mCherry. One HAUS6 construct resistant to shRNA was used in rescue experiments. Briefly, two silent mutations were inserted at Lys123 (G369A) and Ile125 (T375C) by site-directed mutagenesis of pGW2-GFP-HAUS6 described above. To generate Bio-GFP-HAUS2 or HAUS6, HAUS2 and HAUS6 were recloned from pGW2-GFP-HAUS2/6 with AscI/SalI restriction enzymes and inserted in Bio-GFP vector. To generate pGW2-GCP2-mCherry, mCherry was first amplified by PCR and inserted C terminally in a pGW2 vector. Full length human GCP2 RefSeq 902 aa (NCBI:NM_006659.3, UniProt:Q9BSJ2) was amplified by PCR from pGW1-GCP2-GFP (a kind gift from Dr. Kah W. Yau and Dr. Kai Jiang, Department of Cell Biology, University of Utrecht, The Netherlands) and inserted upstream of mCherry in AscI/SalI restriction sites of pGW2-mCherry. The following shRNA constructs were created and used in this study: pSuper mouse HAUS6 shRNA#1 (5'-aggagagagacgttattag-3'), pSuper mouse HAUS6 shRNA#2 (5'-caggctttcagaaactagt -3'), pSuper rat HAUS2 shRNA#1 (HAUS2 KD#1) (5'-gaggagatgttagatatat-3'), pSuper rat HAUS2 shRNA#2 (HAUS2 KD#2) (5'-cgttcagtcaattacatgt-3'), pSuper rat HAUS6 shRNA#1 (HAUS6 KD#1) (5'-gggaaagattatcagatat -3'), pSuper rat HAUS6 shRNA#2 (HAUS6 KD#2) (5'- gtcctaagtttattcatct -3'). shRNA sequences were created with http://sirna.wi.mit.edu/ (Yuan et al., 2004) and oligonucleotides were annealed and inserted in pSuper vector (HindIII/BglII).

**Antibodies and Reagents**
The following antibodies were used in this study: chicken anti-β-galactosidase (Aves Labs BGL-1040, RRID:AB_2313507), chicken anti-MAP2 (Abcam, ab5392, RRID:AB_2138153), mouse anti-dephosphorylated Tau clone PC1C6 (Chemicon, MAB3420, RRID:AB_94855), mouse anti-Acetylated Tubulin (Sigma-Aldrich, T7451, RRID:AB_609894), mouse anti-Ankyrin G clone 4G3F8 (Life Technologies, 33-8800, RRID:AB_2533145), mouse anti-α-Tubulin (Sigma-Aldrich, T5168, RRID:AB_477579), mouse anti-Centrin clone 20H5 (Milipore, 04-1624, RRID:AB_11211820), mouse anti-HA clone 16B12 (Covance, MMS-101P-200, RRID:AB_10064068), mouse anti-MAP2 (Sigma-Aldrich, M9942, RRID:AB_477256), mouse anti-Pan-Neurofascin extracellular (UC Davis/NIH NeuroMab Facility, 75-172, RRID:AB_2282826), rabbit anti-Pericentrin (BioLegend, 923701, RRID:AB_2565440), rabbit anti-EB3 (02-1005-07, (Stepanova et al., 2003)), rabbit anti-GFP (MBL, 598, RRID:AB_591819), rabbit anti-HAUS6 (Uehara et al., 2009), rabbit anti-TRIM46 (van Beuningen et al., 2015), rat anti-Ctip2 (Abcam 18465, RRID:AB_2064130), rat anti-Tubulin Tyrosinated clone YL1/2 (Abcam, ab6160, RRID:AB_305328), rabbit anti-GAPDH (Sigma, G9545, RRID:AB_796208), anti-chicken IgY (IgG) Dyelight 405 (Jackson ImmunoResearch Labs, 703-475-155, RRID:AB_2340373), anti-chicken IgY Alexa568 (Life Technologies, A11041, RRID:AB_2534098), anti-mouse IgG Alexa488 (Life Technologies, A-11029, RRID:AB_2534088), anti-mouse IgG Alexa568 (Life Technologies, A11031, RRID:AB_144696), anti-mouse IgG Alexa647 (Life Technologies, A21236, RRID:AB_2535805), anti-mouse IgG2a Alexa 647 (Life Technologies, A-21241, RRID:AB_2535810), anti-mouse IgG2a Alexa594 (Life Technologies, A-21135, RRID:AB_2535774), anti-rabbit IgG Alexa488 (Life Technologies, A11034, RRID:AB_2576217), anti-rabbit IgG Alexa647 (Life Technologies, A21245, RRID:AB_2535813), anti-rat IgG Alexa488 (Life Technologies, A-11006, RRID:AB_2534074), anti-rat IgG Alexa568 (Life Technologies, A11077, RRID:AB_2534121),  anti-mouse-D2 (Ultivue™-2 super-resolution 2-plex kit, U10001), anti-mouse IRDye800CW (Li-Cor/Westburg, 926-32210, RRID:AB_621842), anti-rat IRDye800CW (Li-Cor/Westburg, 926-32219, RRID:AB_1850025), anti-rabbit IRDye680LT rabbit (Li-Cor/Westburg, 926-68021, RRID:AB_10706309). Other reagents used in this study were: Lipofectamine 2000 (Thermofisher Scientific, 11668019), Polyethylenimine HCl MAX, Linear, MW 40000, Transfection Grade (PEI MAX 40K, Polysciences, 24765-2),

Taxol (Sigma-Aldrich, T7402), Vectashield mounting medium (Vector Labs, H-1000), Vectashield mounting medium with DAPI (Vector Labs, H-1200).

**Immunofluorescence staining and imaging**
For neuron immunocytochemistry cells were fixed for 10 minutes with paraformaldehyde (4%) or for 5 minutes with methanol (100%) at -20°C. Fixed neurons were washed 3 times for 5 minutes in PBS and incubated with primary antibodies in GDB buffer (0.2% BSA, 0.8 M NaCl, 0.5% Triton X-100, 30 mM phosphate buffer, pH 7.4) overnight at 4°C. After 3 times washing with PBS, cells were incubated with secondary antibodies in GDB buffer for 1 hr at room temperature. After washing, coverslips were mounted in Vectashield (VectorLabs) or mowiol. For methanol fixed samples, GDB was used without Triton. Live labelling of the axonal initial segment was performed with an antibody recognizing an extracellular epitope of neurofascin (Pan-Neurofascin extracellular (UC Davis/NIH NeuroMab Facility, 75-172, RRID:AB_2282826). Neurons were incubated with primary antibody in conditioned NB for 10 minutes, washed twice with fresh NB, incubated with a secondary Alexa-conjugated antibody for 8 minutes and washed twice with fresh NB. Extraction, fixation and immunocytochemistry for microtubules was performed as previously described (Chazeau et al., 2016). Briefly, cells were incubated for 90 seconds in extraction buffer preheated at 37°C (80 mM PIPES, 2 mM $MgCl_2$, 1 mM EGTA, 0.3% Triton-X100 and 0.25% glutaraldehyde, pH 6.9), followed by incubation with 4% PFA preheated at 37°C for 10 minutes. Neurons were further permeabilized with 0.25% Triton X-100 and blocking was performed with 2% w/v bovine serum albumin (BSA), 0.2% gelatin, 10 mM glycine, 50 mM $NH_4Cl$ in PBS, pH 7.4. Primary and secondary antibodies were incubated for 1 hr at room temperature in blocking buffer. For SMLM (single-molecule localization microscopy), the same immunocytochemistry protocol was performed under the microscope using the secondary antibody anti-mouse-D2 and buffers from the Ultivue™-2 (super-resolution 2-plex kit). Cells with low expression levels of the different constructs were used in all the analysis. To visualize actin in SMLM, LifeAct-GFP was purified and used as a transient binding probe as previously described (Kiuchi et al., 2015; Tas et al., 2018).
Brain sections were obtained from embryos at E17.5 and fixed in 4% paraformaldehyde followed by submersion in 30% sucrose. Brains were placed in Jung tissue freezing medium (Leica) and cut in 12 μm coronal sections. Cryosections were blocked and permeabilized with 10% normal goat serum in 0.2% Triton X-100 PBS (Blocking buffer) for 1 hr followed by incubation with primary antibody diluted in blocking buffer overnight at 4°C. After washing, sections were incubated with secondary antibody diluted in blocking buffer for 90 minutes and mounted using Vectashield mounting medium containing DAPI (Vectorlabs).
IMCD3 cells were fixed for 5 minutes in methanol at -20°C. Fixed cells were washed 3 times in PBS following blocking and permeabilization with 2% BSA supplemented with 0.05% Tween-20 in PBS (Blocking buffer) for 20 minutes. Primary antibodies were diluted in blocking buffer and incubated overnight at 4°C. Secondary antibodies diluted in 0.05% Tween-20 in PBS (washing solution) were incubated with samples for 1 hr at room temperature after three rounds of washing. After washing 3 times in washing solution and a final wash in MilliQ, samples were mounted with Vectashield mounting medium with DAPI (Vectorlabs).
Imaging of fixed neurons or cell lines was performed using Confocal laser scanning microscopy with a Zeiss LSM700 confocal laser-scanning microscope with a Plan-Apochromat 63× N.A. 1.40 oil DIC, EC Plan-Neofluar 40× N.A. 1.30 Oil DIC and a Plan-Apochromat 20× N.A. 0.8 objective using 405 nm, 488 nm, 555 nm, and 633 nm laser lines. Confocal images of brain slices were acquired using a Zeiss LSM700 with a 20× N.A. 0.5 objective (for migration analysis) or a 40× N.A. 0.8 (for morphology analysis) using 405 nm, 488 nm, 555 nm, and 633 nm laser lines. A total thickness of 15 μm in 1 μm steps was scanned for each position, and maximum intensity projections were generated for analysis. To access the entire brain slice, four images were taken side by side and image stitching was performed using ZEN 2011 Software. The degree of neuronal migration was quantified as described previously (Hand et al., 2005).

**Live imaging**
Live imaging of neurons was performed using spinning-disk confocal microscopy with an inverted microscope Nikon Eclipse Ti-E incorporated with a Plan Apo VC 100× N.A. 1.40 oil objective, or a Nikon Eclipse TE2000E equipped with CFI Apo TIRF 100× N.A. 1.49; both microscopes are equipped with a Perfect Focus System, a Yokogawa CSU-X1-A1 spinning-disk confocal unit, an Evolve 512 EMCCD camera (Photometrics), and a motorized XYZ stage (Applied Scientific Instrumentation) which were all controlled using MetaMorph (Molecular Devices) software.
Three color SMLM was performed on a Nikon Ti microscope equipped with a 100× N.A. 1.49 Apo TIRF oil objective, a Perfect Focus System and an additional 2.5× Optovar to achieve an effective pixel size of 64 nm. Oblique laser illumination was achieved using a custom illumination pathway with a 15 mW 405 nm diode laser (Power Technology), a 50 mW 491 nm DPSS laser (Cobalt Calypso) and a 40 mW 640 nm diode laser (Power Technology). Fluorescence was detected using a water-cooled Andor DU-897D EMCCD camera and ET series Cy5 filter (Chroma Technology). All components were controlled by μManager software (Edelstein et al., 2010). After immunocytochemistry, samples were first incubated for 15

minutes with Tetraspeck™ 100 nm-beads (Invitrogen). High laser power induced blinking of GFP-HAUS2 was first imaged for 1000-2000 frames, after which it was completely bleached. LifeAct-GFP and fluorescently labelled DNA complementary strand, I2-650 (binding to anti-mouse-D2) were then added and diluted to obtain single molecule binding events. DNA-PAINT imaging was performed according to Ultivue™-2 super-resolution 2-plex kit protocol. Subsequently, LifeAct-GFP was imaged as previously described (Janssen et al., 2017). Between 20,000 and 30,000 frames were recorded per acquisition with exposure time of 100 ms.

## Drug treatments
Where indicated, neurons were treated with 10 nM Taxol (Sigma) for 48 hrs.

## Western blot
Cortical neuron lysates were prepared at DIV4 by scraping cells directly in sample buffer (4% SDS, 20% glycerol, 100 mM Tris pH 6.8, 200 mM DTT and 20 mg/l bromophenol blue). Samples were boiled at 99º C for 10 minutes and centrifuged at 16000 g before being analyzed by SDS-PAGE. Proteins were transferred to PVDF membranes (Millipore) using a wet blotting system (Bio-Rad). Membranes were blocked and incubated with primary antibodies (overnight at 4°C) in blocking buffer containing 3% BSA in PBS-T (PBS1x, 0.1% Tween-20). After three 10 minute washing steps in PBS-T membranes were incubated with secondary antibodies in blocking buffer for 1 hr at room temperature. Membranes were scanned using Odyssey infrared imaging system (Li-COR Biosciences). The relative intensities of $\alpha$-, tyrosinated and acetylated tubulin were obtained by normalization to the GAPDH loading control. The relative intensity of each tubulin after HAUS6 knockdown was then normalized to the corresponding control. Quantifications were performed in Fiji (Schindelin et al., 2012).

## Affinity Purification-Mass Spectrometry
Streptavidin beads pull-down assays were performed with HEK293 cells transfected with BirA and Bio-GFP-HAUS2, Bio-GFP-HAUS6 and Bio-GFP using polyethylenimine (PEI, Polysciences) for 48 hrs according to the manufacturer's instructions. Cells were lysed in RIPA lysis buffer (50 mM TrisHCl pH 7.4-7.8, 150 mM NaCl, 1% Triton X-100, 0.1% SDS, 0.5% Sodium Deoxycholate) and Protease inhibitors (Roche) for 30 minutes, centrifuged at 17949 g/rcf for 15 minutes at 4ºC and the supernatants incubated with Dynabeads M-280 blocked in chicken egg albumin (Life Technologies) for 1 hr at 4ºC. Beads were separated using a magnet rack (Dynal, Invitrogen) and washed five times in washing buffer (20 mM Tris-HCl pH 7.4-7.8, 150 mM KCl, 0.1% Triton X-100). Samples were collected at this point for AP-MS analysis of HEK293 cells expressing each construct. To sample for brain putative interactors of HAUS2 or HAUS6 pre-incubated Dynabeads with HEK293 cell extracts expressing each construct were washed twice in low salt washing buffer (20 mM Tris-HCl pH 7.4-7.8, 100 mM KCl, 0.1% Triton X-100), followed by two wash steps in high salt wash buffer (20 mM Tris-HCl pH 7.4-7.8, 500 mM KCl, 0.1% Triton X-100) and two final wash steps in low salt washing buffer to remove binding proteins from HEK293 cells. Brains were obtained from female adult rats and homogenized in 10x volume/weight in tissue lysis buffer (50 mM TrisHCl, 150 mM NaCl, 0.1% SDS, 0.2% NP-40, and protease inhibitors (Roche)). Brain lysates were centrifuged at 17494 g/rcf for 10 minutes at 4°C and the supernatant was incubated with the Dynabeads containing Bio-GFP-HAUS2, Bio-GFP-HAUS6 or Bio-GFP for 2 hrs at 4ºC and washed in wash buffer five times. For mass spectrometry analysis, beads were resuspended in 15 μL of 4x Laemmli sample buffer (Bio-Rad) and supernatants were loaded on a 4-12% gradient Criterion XT Bis-Tris precast gel (Bio-Rad). The gel was fixed with 40% methanol and 10% acetic acid and then stained for 1 hr using colloidal coomassie dye G-250 (Gel Code Blue Stain Reagent, Thermo Scientific). Each lane from the gel was cut in 3 slices, destained and digested using trypsin, as described previously (Ekkebus et al., 2013). Briefly, each lane from the gel was cut into three pieces and placed in 0.5-mL tubes. They were washed with 250 μL of water, followed by 15 minutes dehydration in acetonitrile. Proteins were reduced (10 mM dithiothreitol, 1 hr at 56°C), dehydrated and alkylated (55 mM iodoacetamide, 1 hr in the dark). After two rounds of dehydration, trypsin (Promega) was added to the samples (20 μL of 0.1 mg/mL trypsin in 50 mM Ammonium bicarbonate) and incubated overnight at 37°C. Peptides were extracted with acetonitrile, dried down and reconstituted in 10% formic acid prior mass spectrometry analysis.

## Image analysis

No specific strategy for randomization and/or stratification was employed. The studies were blind in data analysis.

## Quantification of immunofluorescence intensity
Images were acquired with a Zeiss LSM700 confocal microscope covering the entire neuron from top to bottom. Recording settings were kept the same for all conditions in each experiment. Only the planes that include the region of interest (ROI) were used for analysis. For quantification of signal intensity in dendrites ROIs within the first 10 μm were manually drawn in

proximal dendrites using Fiji (Schindelin et al., 2012). Mean intensity was measured from these regions and background values were subtracted. For quantification of signal intensity at the centrosome the mean intensity of HAUS6 at each centriole was quantified in average intensity projection images of selected planes by drawing ROIs of 0.3 μm radius encircling each centriole using Fiji. Background subtraction was performed by subtracting the mean intensity of the HAUS6 signal in the area juxtaposed to the centriole with ROIs of 0.3 μm radius from the mean intensity at the centriole. Quantification of HAUS6 at the centrosome for each neuron was obtained with the average of mean intensity of both centrioles.

**Analysis of neuronal morphology**
For analysis of axon development pβactin-GFP or pβactin-HA-β-galactosidase were used as a fill. The axon was identified based on morphology and the presence of AnkG marker in one neurite. Images were acquired with a Zeiss LSM700 confocal microscope. Only neurons with clearly defined neuronal arborisation were imaged and analysed. Total axonal length that includes the length of the longest branch and its branches was quantified with ImageJ software and NeuronJ plugin (Meijering et al., 2004). For analysis of dendritic development pβactin-GFP or pβactin-HA-β-galactosidase were used as a fill. The dendritic arbour was identified based on morphology, and the absence of AnkG marker used to label the axon. Images were acquired with a Zeiss LSM700 confocal microscope. Dendritic arbours were manually labelled in maximum intensity projection images using the Fiji plugin NeuronJ (Meijering et al., 2004). Analysis was performed based on the imported tracing data using the Sholl Analysis plugin v3.4.5 (Ferreira et al., 2014). The first circle was defined by the soma size and subsequent circles with increased 10 μm steps up to 100 μm distance from the cell body. Only branches longer than 8 μm were included in this analysis.

**Quantification of EB3 comets**
Images were acquired with a Zeiss LSM700 confocal microscope covering the entire neuron from top to bottom. Recording settings were kept the same for all conditions in each experiment. ROIs of approximately 10 μm long were manually drawn in proximal dendrites using Fiji (Schindelin et al., 2012). ImageJ plugin ComDet v.0.2.0 (GitHub: https://github.com/ekatrukha/ComDet) was used to quantify the number of EB3 comets in 10 μm proximal dendrites.

**Colocalization and cluster analysis**
Neurons expressing GFP-HAUS2 or GFP-HAUS2 with mCherry-HAUS6 or GCP2-mCherry (colocalization experiments) were imaged with spinning-disk confocal microscopy at 10 frames/second. Analysis of clusters was performed with the average intensity projection of 10 frames. GFP-HAUS2 clusters were quantified using the ImageJ plugin ComDet v.0.3.7 (GitHub: https://github.com/ekatrukha/ComDet). Numbers were normalized to the corresponding area. Colocalization was quantified as the percentage of mCherry-HAUS6 or GCP2-mCherry visually overlapping with GFP-HAUS2.

**Quantification of moving clusters**
Neurons expressing GFP-HAUS2 were imaged with spinning-disk confocal microscopy. Each neuron was imaged for 60 second at 5 frames/second. Run length, time and velocity of GFP-HAUS2 clusters were quantified from 60 second kymographs of proximal dendrites (25 μm) created using the Kymoreslicewide (GitHub: https://github.com/ekatrukha/KymoResliceWide) plugin with Fiji (Schindelin et al., 2012). The percentage of mobile *versus* immobile clusters was quantified in 20 second periods and averaged over a total of 60 seconds for each dendrite. The percentage of retrograde (to the soma) *versus* anterograde (to the dendrite) moving clusters was quantified over 60 second period for each dendrite.

**Quantification of microtubule dynamics**
GFP-MT+TIP marker was co-expressed with a HAUS6 shRNA (HAUS6 KD#2) or pSuper control for 96 hrs prior to spinning-disk confocal imaging. Each middle axon or dendrite (after a first or a second branch point) was imaged for 10 minutes at 1 frame/second. Recordings were low-pass filtered and subtracted with a sliding 10 frame average projection (Schatzle et al., 2016). Comet orientation was determined from a 10 minute kymograph created using the Kymoreslicewide (GitHub: https://github.com/ekatrukha/KymoResliceWide) plugin with Fiji (Schindelin et al., 2012). Starting and end positions of the traces were marked by the "Cell Counter" plugin, and coordinates were exported to determine the percentage of retrograde (to the soma) *versus* anterograde (to the dendrite or axon).

**Quantification of mitotic defects**

IMCD3 cells were imaged with a Zeiss LSM700 confocal microscope covering the cells from top to bottom. Cells in mitosis or with abnormal spindles were identified based on α-tubulin staining. The percentage of cells in mitosis (mitotic index) and the percentage of abnormal spindles were quantified in cells depleted for HAUS6 and compared with controls.

**Mass spectrometry analysis**
All samples were analysed on an Orbitrap Q-Exactive mass spectrometer (Thermo Fisher Scientific, Bremen, Germany) coupled to an Agilent 1290 Infinity LC (Agilent Technologies). Peptides were loaded onto a trap column (Reprosil C18, 3 μm, 2 cm × 100 μm; Dr. Maisch) with solvent A (0.1% formic acid in water) at a maximum pressure of 800 bar and chromatographically separated over the analytical column (Zorbax SB-C18, 1.8 μm, 40 cm × 50 μm; Agilent) using 90 min linear gradient from 7-30% solvent B (0.1% formic acid in acetonitrile) at a flow rate of 150 nL/min. The mass spectrometer was used in a data-dependent mode, which automatically switched between MS and MS/MS. After a survey scan from 350-1500 m/z the 10 most abundant peptides were subjected to HCD fragmentation. MS spectra were acquired in high-resolution mode (R > 30,000), whereas MS2 was in high-sensitivity mode (R > 15,000). For data analysis, raw files were processed using Proteome Discoverer 1.4 (version 1.4.1.14, Thermo Scientific, Bremen, Germany). Database searches were performed either using the human Uniprot database or the rat Uniprot database and Mascot (version 2.5.1, Matrix Science, UK) as the search engine. Carbamidomethylation of cysteines was set as a fixed modification and oxidation of methionine was set as a variable modification. Trypsin was set as cleavage specificity, allowing a maximum of 2 missed cleavages. Data filtering was performed using percolator, resulting in 1% false discovery rate (FDR). Additional filters were search engine rank 1 and mascot ion score >20.

**Map of interactions analysis**
Gene ontology (GO) classification was obtained via PANTHER (Mi et al., 2005). Selected HAUS2 and HAUS6 interactors linked to microtubule cytoskeleton or actin cytoskeleton were used for the generation of protein-protein interaction networks in Figure S4B. Network analyses were performed using the GeneMania plugin (Montojo et al., 2010) within Cytoscape (Shannon et al., 2003). Edge color coding: blue, colocalization; orange, predicted interaction; green, shared protein domain; purple, co-expression.

**Gene ontology analysis**
The percentage of occurrence of actin, microtubule cytoskeleton and cytoskeleton groups within the interactors of Bio-GFP-HAUS2 and HAUS6 was calculated. For the analysis the top 100-150 hits were selected and classified using g:Profiler (Reimand et al., 2016).

**Supplemental References**
Brummelkamp, T.R., Bernards, R., and Agami, R. (2002). A system for stable expression of short interfering RNAs in mammalian cells. Science (New York, NY) 296, 550-553.

Chazeau, A., Katrukha, E.A., Hoogenraad, C.C., and Kapitein, L.C. (2016). Studying neuronal microtubule organization and microtubule-associated proteins using single molecule localization microscopy. Methods Cell Biol 131, 127-149.

Dittgen, T., Nimmerjahn, A., Komai, S., Licznerski, P., Waters, J., Margrie, T.W., Helmchen, F., Denk, W., Brecht, M., and Osten, P. (2004). Lentivirus-based genetic manipulations of cortical neurons and their optical and electrophysiological monitoring in vivo. Proceedings of the National Academy of Sciences of the United States of America 101, 18206-18211.

Edelstein, A., Amodaj, N., Hoover, K., Vale, R., and Stuurman, N. (2010). Computer control of microscopes using microManager. Current protocols in molecular biology Chapter 14, Unit14.20.

Ekkebus, R., van Kasteren, S.I., Kulathu, Y., Scholten, A., Berlin, I., Geurink, P.P., de Jong, A., Goerdayal, S., Neefjes, J., Heck, A.J., *et al.* (2013). On terminal alkynes that can react with active-site cysteine nucleophiles in proteases. J Am Chem Soc 135, 2867-2870.

Ferreira, J.P., Overton, K.W., and Wang, C.L. (2013). Tuning gene expression with synthetic upstream open reading frames. Proceedings of the National Academy of Sciences of the United States of America 110, 11284-11289.

Ferreira, T.A., Blackman, A.V., Oyrer, J., Jayabal, S., Chung, A.J., Watt, A.J., Sjostrom, P.J., and van Meyel, D.J. (2014). Neuronal morphometry directly from bitmap images. Nat Methods 11, 982-984.

Goslin, K., and Banker, G. (1989). Experimental observations on the development of polarity by hippocampal neurons in culture. The Journal of cell biology 108, 1507-1516.

Hand, R., Bortone, D., Mattar, P., Nguyen, L., Heng, J.I., Guerrier, S., Boutt, E., Peters, E., Barnes, A.P., Parras, C.*, et al.* (2005). Phosphorylation of Neurogenin2 specifies the migration properties and the dendritic morphology of pyramidal neurons in the neocortex. Neuron 48, 45-62.

Hoogenraad, C.C., Milstein, A.D., Ethell, I.M., Henkemeyer, M., and Sheng, M. (2005). GRIP1 controls dendrite morphogenesis by regulating EphB receptor trafficking. Nat Neurosci 8, 906-915.

Janssen, A.F.J., Tas, R.P., van Bergeijk, P., Oost, R., Hoogenraad, C.C., and Kapitein, L.C. (2017). Myosin-V Induces Cargo Immobilization and Clustering at the Axon Initial Segment. Front Cell Neurosci 11, 260.

Jaworski, J., Kapitein, L.C., Gouveia, S.M., Dortland, B.R., Wulf, P.S., Grigoriev, I., Camera, P., Spangler, S.A., Di Stefano, P., Demmers, J.*, et al.* (2009). Dynamic microtubules regulate dendritic spine morphology and synaptic plasticity. Neuron 61, 85-100.

Kapitein, L.C., Schlager, M.A., van der Zwan, W.A., Wulf, P.S., Keijzer, N., and Hoogenraad, C.C. (2010a). Probing intracellular motor protein activity using an inducible cargo trafficking assay. Biophys J 99, 2143-2152.

Kapitein, L.C., Yau, K.W., and Hoogenraad, C.C. (2010b). Microtubule dynamics in dendritic spines. Methods Cell Biol 97, 111-132.

Kiuchi, T., Higuchi, M., Takamura, A., Maruoka, M., and Watanabe, N. (2015). Multitarget super-resolution microscopy with high-density labeling by exchangeable probes. Nat Methods 12, 743-746.

Meijering, E., Jacob, M., Sarria, J.C., Steiner, P., Hirling, H., and Unser, M. (2004). Design and validation of a tool for neurite tracing and analysis in fluorescence microscopy images. Cytometry Part A : the journal of the International Society for Analytical Cytology 58, 167-176.

Mi, H., Lazareva-Ulitsky, B., Loo, R., Kejariwal, A., Vandergriff, J., Rabkin, S., Guo, N., Muruganujan, A., Doremieux, O., Campbell, M.J.*, et al.* (2005). The PANTHER database of protein families, subfamilies, functions and pathways. Nucleic Acids Res 33, D284-288.

Montojo, J., Zuberi, K., Rodriguez, H., Kazi, F., Wright, G., Donaldson, S.L., Morris, Q., and Bader, G.D. (2010). GeneMANIA Cytoscape plugin: fast gene function predictions on the desktop. Bioinformatics (Oxford, England) 26, 2927-2928.

Reimand, J., Arak, T., Adler, P., Kolberg, L., Reisberg, S., Peterson, H., and Vilo, J. (2016). g:Profiler-a web server for functional interpretation of gene lists (2016 update). Nucleic Acids Res 44, W83-89.

Schatzle, P., Kapitein, L.C., and Hoogenraad, C.C. (2016). Live imaging of microtubule dynamics in organotypic hippocampal slice cultures. Methods Cell Biol 131, 107-126.

Schindelin, J., Arganda-Carreras, I., Frise, E., Kaynig, V., Longair, M., Pietzsch, T., Preibisch, S., Rueden, C., Saalfeld, S., Schmid, B.*, et al.* (2012). Fiji: an open-source platform for biological-image analysis. Nat Methods 9, 676-682.

Shannon, P., Markiel, A., Ozier, O., Baliga, N.S., Wang, J.T., Ramage, D., Amin, N., Schwikowski, B., and Ideker, T. (2003). Cytoscape: a software environment for integrated models of biomolecular interaction networks. Genome research 13, 2498-2504.

Tas, R.P., Bos, T., and Kapitein, L.C. (2018). Purification and Application of a Small Actin Probe for Single-Molecule Localization Microscopy. Methods Mol Biol 1665, 155-171.

Tortosa, E., Adolfs, Y., Fukata, M., Pasterkamp, R.J., Kapitein, L.C., and Hoogenraad, C.C. (2017). Dynamic Palmitoylation Targets MAP6 to the Axon to Promote Microtubule Stabilization during Neuronal Polarization. Neuron 94, 809-825 e807.

Yuan, B., Latek, R., Hossbach, M., Tuschl, T., and Lewitter, F. (2004). siRNA Selection Server: an automated siRNA oligonucleotide prediction server. Nucleic Acids Res 32, W130-134.